Mycorrhiza (2001) 10:209–215

ORIGINAL PAPER

J.M. Arocena · K.R. Glowa · H.B. Massicotte

Calcium-rich hypha encrustations on *Piloderma*

Accepted: 15 October 2000

Abstract *Piloderma* species are broad-host-range fungi associated with a wide variety of conifer and hardwood species to form ectomycorrhizae (ECM). In this study, we investigated the hypha crystals collected from *Piloderma* – *Picea glauca* × *engelmannii* ECM as an initial step in the elucidation of the role of mycorrhizal fungi in mineral weathering and nutrient cycling. We compared the morphology and composition of hypha encrustation between field and cultured *Piloderma* samples. For field samples, the morphology of encrustations was dominated by elongated crystals often underlain by verrucose crystals. Cultured samples had mostly verrucose crystals. Generally, encrustations on field samples had higher calcium contents than cultured samples. Calcium contents ranged from 3% in the verrucose crystals of cultured samples to 17% in verrucose and elongated crystals of field samples. Encrustations had infrared absorption bands at 1333 and 781 cm^{-1} wavenumbers, indicative of the presence of oxalate. High amounts of C and O in verrucose crystals are likely associated with the crystal sheath around all encrustations. This composition suggests an intracellular origin for the crystals. It is possible that encrustations start as verrucose crystals and develop into euhedral elongated crystals susceptible to dislodgement into the soil environment. These crystals may prevent the desiccation of the hyphae and inhibit the build-up of calcium and oxalate in fungus cells.

Keywords Electron microscope · Infrared · Hybrid white spruce

J.M. Arocena (✉) · K.R. Glowa · H.B. Massicotte
Forestry Program, Faculty of Natural Resources and Environmental Studies,
University of Northern British Columbia,
Prince George, BC, Canada V2N 4Z9
e-mail: arocenaj@unbc.ca
Tel.: +1-250-9605811, Fax: +1-250-9605538

Introduction

Piloderma is one of the most noticeable genera of ectomycorrhizal fungi in cool temperate and boreal forests because of its bright yellow color and wide distribution in North America and Europe. For instance, *Piloderma fallax* (= *P. bicolor* = *P. croceum;* see Larsen et al. 1997) is rhizomorphic, clampless, with a bright saffron yellow color (near 2.5Y 8/10 in Munsell notation) and finely verrucose hyphae with H-shaped anastomoses (Agerer 1987–1998; Goodman and Trofymow 1996). Some *Piloderma* species can grow in pure culture and, consequently, have been used in synthesis and physiology experiments (Nylund 1981, 1987; Nylund and Unestam 1982; Massicotte et al. 1993). Because of its distribution and growth characteristics, *Piloderma* is an ideal candidate for in situ ecological studies (Larsen et al. 1997; Wallander et al. 1997; Goodman and Trofymow 1998; Arocena et al. 1999).

Piloderma species are broad-host-range fungi associated with a wide variety of conifer and hardwood species to form ectomycorrhizae (ECM) (Molina et al. 1992). These ectomycorrhizal systems are found in decaying wood and fragmented litter (Zak 1976; Nylund 1981; Goodman and Trofymow 1996) and in acid humus under litter and moss (Agerer 1987–1998), but seldom in mineral soil (Goodman and Trofymow 1996). A taxonomic analysis of *Piloderma* sporocarps (Larsen et al. 1997) indicated their presence in rotten or decorticated wood, under mosses, among roots, and in the litter layer. Recently, we described *Piloderma* ECM of *Abies lasiocarpa* in the LFH/Ae boundary of Luvisolic soils in central British Columbia (Arocena et al. 1999).

Like other ECM, *Piloderma* influences nutrient uptake and modifies soil mineral weathering, especially in the ectomycorrhizosphere, i.e., the soil environment in the immediate vicinity of the ECM (Paris et al. 1994, 1995a, b, 1996; Jongmans et al. 1997; Arocena et al. 1999). For instance, in granitic rocks in Sweden, *Piloderma croceum* hyphae connect calcium feldspars and tree roots, thereby participating directly in tree nutrition

(Jongmans et al. 1997). Recently, we documented that the cation exchange capacity, exchangeable Ca, Mg, and K in ectomycorrhizosphere soils dominated by *Piloderma* were higher than in non-ectomycorrhizosphere soils of *Abies lasiocarpa* (Arocena et al. 1999). The transformation of mica and chlorite to 2:1 expandable clays appeared pronounced in *Piloderma*-dominated soils, likely because of the high production of organic acids and direct extraction of K and Mg by *Piloderma* hyphae (Arocena et al. 1999).

The presence of crystalline materials encrusted on *Piloderma* hyphae is characteristic and these can be of different shapes (Larsen et al. 1997). Verrucose (Goodman and Trofymow 1996), grainy due to corticrocin (Agerer 1987–1998; Brand 1991), and needle-shaped (Agerer 1987–1998) are qualifiers often used to describe these hyphal ornaments. Crystalline encrustations have been reported for other species of mycorrhizal fungi such as *Hysterangium crassum* (Cromack et al. 1979), as well as unidentified fungi colonizing *Monotropa uniflora* roots (Snetselaar and Whitney 1990), *Paxillus involutus* (Lapeyrie et al. 1990), and several *Suillus* (Danielson 1991) and *Rhizopogon* species (Massicotte et al. 1999). Non-mycorrhizal fungi such as *Agaricus bisporus* (Whitney and Arnott 1987), *Geastrum saccatum* (Whitney and Arnott 1986a), and *Resinicium bicolor* (Connolly and Jellison 1994) have also been reported to have crystalline hyphal deposits. Connolly and Jellison (1994) described the encrustations as druses of twinned crystals of calcium monohydrate that are more birefringent than calcium dihydrate minerals. Whitney and Arnott (1987) indicated that the encrustations were acicular and elongated and made up of plate-like crystals arranged tangentially to hyphal surfaces.

The accumulation of calcium in these crystals has been reported to be as high as 82 g calcium oxalate per square meter of soil with *Hysterangium crassum* under Douglas-fir (Cromack et al. 1979). Snetselaar and Whitney (1990) hypothesized that *Monotropa uniflora* mycorrhizae accumulate calcium oxalate to avoid potential toxicities and phosphorus deficiency due to the reaction of calcium with phosphorus. Graustein et al. (1977) also elaborated on the significant influence of calcium oxalate crystals on nutrient cycles in natural ecosystems.

In order to better understand the contribution of fungus crystals to nutrient cycles as well as to tree nutrition in northern forest ecosystems, this study compares the morphological and chemical properties of hyphal encrustations on *Piloderma* sp. grown in vitro to *Piloderma* ECM of hybrid white spruce (*Picea glauca* × *engelmannii*) occurring in Gray Luvisolic soils in the central interior of British Columbia, Canada.

Materials and methods

Description of the study area and sample collection

The study area is within the Sub-Boreal Spruce biogeoclimatic zone (Meidinger et al. 1991) in the central interior of British Columbia, near the campus of the University of Northern British Columbia in Prince George (53° 54”N 123° 49’W). The soil is a Brunisolic Gray Luvisol (Dawson 1989) developed on drumlinized basal till with a 4-cm-thick forest floor and an approximately 10-cm-thick Ae horizon. The annual precipitation ranges from 500 to 800 mm and mean annual temperature is 3.3°C. Vegetation is dominated by hybrid white spruce *(Picea glauca* × *engelmannii),* subalpine fir *(Abies lasiocarpa),* and lodgepole pine (*Pinus contorta* var. *latifolia)* with minor amounts of Douglas-fir *(Pseudotsuga menziesii*), trembling aspen (*Populus tremuloides*), cottonwood (*P. balsamifera* var. *trichocarpa),* and paper birch (*Betula papyrifera*), with a mixture of shrubs as the understory vegetation.

Samples of *Piloderma* ECM were collected during the summer of 1998 at the base of four mature hybrid white spruce trees. ECM were collected after removing the humus layer from a sampling quadrat approximately 2 m by 2 m at the base of each tree to expose the rooting zone in the LFH/Ae horizon boundary. Roots were carefully selected by tracing the rootlets to the main roots of hybrid white spruce. After verification that the roots were linked, roots with predominant *Piloderma* colonization were collected, placed in plastic bags and stored at 4°C until processing. *Piloderma* collected from field samples of *Picea* roots are referred to as field samples.

Mycorrhiza description

The rootlets were washed with deionized water, placed in a glass dish and described morphologically following the guidelines outlined by Goodman and Trofymow (1996), Ingleby et al. (1990), and Agerer (1987–1998). Mycorrhizal tips were selected, examined microscopically, and characterized according to their branching pattern, surface texture, luster, color, mantle characteristics, emanating hyphae, and other morphological properties. Permanent slide mounts, photographs, and frozen samples were kept for future reference.

Piloderma cultures

Within 6 h of field collection, 120–150 root tips with healthy-looking ECM of *Piloderma* were washed, kept immersed in cold deionized water, and stored at 4°C before plating. Each root tip with ECM was surface sterilized by dipping in 85% ethanol (1–2 s), soaking in 30% H_2O_2 for approximately 15±10 s, and rinsed three times in sterile deionized water for 50±30 s (Danielson 1984). Three to four ECM were then placed on each of five petri plates of either modified Melin-Norkrans medium (MMN) (Marx 1969) or potato dextrose agar (Difco), each with the addition of 100 ppm streptomycin, 50 ppm chlorotetracycline, and 2–5 ppm Benomyl. Plates were incubated at room temperature (20–25°C) for 3–4 months. When bright yellow fungus growth was observed emanating from the root tips, isolates were re-cultured in MMN without antibiotics and fungicides. Once cultures had grown over half of a plate, they were stored at 4°C. Two of these pure cultures were examined for the presence of encrustations and are referred to as cultured samples.

Reference samples of hydrated calcium oxalate crystal

Crystals of calcium oxalate were prepared as a reference for the mineral composition of the *Piloderma* encrustations. Hydrated calcium oxalate was crystallized from a mixture of equal amounts of 1 M CaOH and 1 M oxalic acid. Crystals formed from this mixture after 2 days at room temperature.

Electron microscopy and in situ chemical analysis

The submicroscopic surface morphology of *Piloderma* encrustations was examined using a Philips XL30 scanning electron mi-

croscope equipped with an EDAX energy dispersive system (SEM-EDS). *Piloderma* hyphae from field and cultured samples were freeze dried and mounted onto aluminum stubs using double-sided tape, then sputter-coated with Au for 60 s prior to SEM-EDS analysis. Once Au-coated, the morphology of the crystal encrustation was examined under SEM while the semi-quantitative chemical composition was determined using standardless EDS technique. The mean corrected (*Z* atomic number, *A* absorption, and *F* fluorescence factors) elemental composition was determined from an energy dispersive spectrum collected for 200 s with an electron beam of 1 µm from ten encrustations in each of the field and cultured samples.

For transmission electron microscopy (TEM), field samples of *Piloderma* ECM were fixed overnight at 6°C in 2.5% glutaraldehyde in HEPES buffer (Massicotte et al. 1986). Samples were postfixed in 2% osmium tetroxide for 2 h, dehydrated in a graded ethanol series and embedded in Araldite CY212 mixture. Several thin sections of the hyphae and their encrustations were obtained using an Ultracut E ultrathin section microtome. Six sections from three field samples and at least eight sections from two cultured samples were observed using a Hitachi transmission electron microscope H-7000.

Fourier transformed infrared analysis

Infrared analysis was conducted to determine the mineral composition of the encrustations using a Perkin Elmer Fourier transformed infrared spectrometer (FTIR). A KBr pellet composed of approximately 1:100 ratio of encrustations to KBr was prepared by pressing the mixture with a manual press. The KBr pellet was subjected to an IR beam for about 1 min and the interferogram was recorded from 400–2000 cm^{-1} wavenumber. A similar procedure was followed for the analysis of reference crystals of hydrated calcium oxalate and the encrustations from cultured and field samples. Two KBr pellets from each type of sample were used.

Statistical analysis

We analyzed the data by ANOVA using Statistica 5 (Statsoft 1995). The distribution of data was checked for normality using the Shapiro-Wilks *W*-test statistic and for homogeneity of variance using Levene's test. Post hoc comparison of significantly different means was made using Tukey's honest significant difference test.

Results

Description of field and cultured samples of *Piloderma* ectomycorrhizae

Field ECM were characterized as being bright yellow, felty to cottony, with a felt prosenchyma outer mantle and abundant undifferentiated mycelial strands. Emanating hyphae were 1.5–2.5 µm wide, clampless, with numerous septa and H-shaped anastomoses. Hyphae were covered with verrucose crystals overlain by 3-to 5-µm-long crystals of lenticular and elongated morphologies. These distinguishing characteristics are similar to those described for *Piloderma* by Agerer (1987–1998), Ingleby et al. (1990), Goodman and Trofymow (1996) and Arocena et al. (1999).

Piloderma in pure culture grown on MMN was bright yellow (2.5Y 8/8) (Munsell color chart) and exhibited a cotton-like growth over the agar surface with rare H-shaped anastomoses and rhizomorphic growth. The hyphae (2–3 µm wide, septate) were encrusted with copious verrucose crystals and many lenticular or elongated crystals. Elongated crystals can be as abundant as 10–14 per 10-µm length of hyphae, but usually 0–4 occur randomly and sporadically.

Morphology of *Piloderma* encrustations

The encrustations on the hyphae of *Piloderma* from both field and cultured samples in the present study can be described as euhedral, i.e., crystals completely bounded by crystal faces (Bullock et al. 1985). We observed two general morphologies of crystals: verrucose, ranging from 0.2 to 1.0 µm in width (Fig. 1 a, b, d, g, h), and lenticular or elongated about 4–7 µm long (Fig. 1a, e–h). The verrucose type covered most of the external surface of the hyphae (Fig. 1b, c, d, g, h), whereas the lenticular or elongated types appeared to accumulate over the verrucose crystals (Fig. 1d, g, h). The elongated crystals were tangentially attached and tapered from about 1.0 µm at their base to less than 0.5 µm at the distal end. There appeared to be some regularity in the occurrence of elongated crystals every 4–6 µm (Fig. 1f–h). When *Piloderma* hyphae were kept in water, the water turned yellow after a few seconds, especially with hyphae from cultured samples. The occurrence of elongated encrustations in cultured *Piloderma* appeared less dense than in field samples.

Transmission electron micrographs of cross-sections of fungus hyphae revealed the presence of elongated (Fig. 2a) and verrucose (Fig. 2b) encrustations outside the cell wall. The elongated encrustations were angular and coated with electron-dense materials. The coating or "crystal sheath" was about 0.07 µm thick and exhibited a laminated morphology similar to that of the hypha wall (Figs. 2b, d). Verrucose crystals showed a thicker crystal sheath than the elongated, euhedral crystals. The presence of inner membrane organelles was noticeable in association with the encrustations (Fig. 2c).

Element composition of encrustations

Energy dispersive analysis revealed the element composition of encrustations to be predominantly of C, O, Al, Si, K, Ca, and Fe (Table 1). Field verrucose encrustations had a lower C and higher O content than encrustations from pure culture. Field elongated crystals had significantly higher O and lower C contents than verrucose types. The C and O contents of crystals from pure culture were not significantly different between the two types. The Al, Si, K, and Fe contents were less than 2% (weight) and were not significantly different between the two types of encrustation, regardless of source. Ca content ranged from 3% in the verrucose type in cultured samples to 17% in both types in field samples. Generally, encrustations on field samples had a higher Ca content than cultured samples.

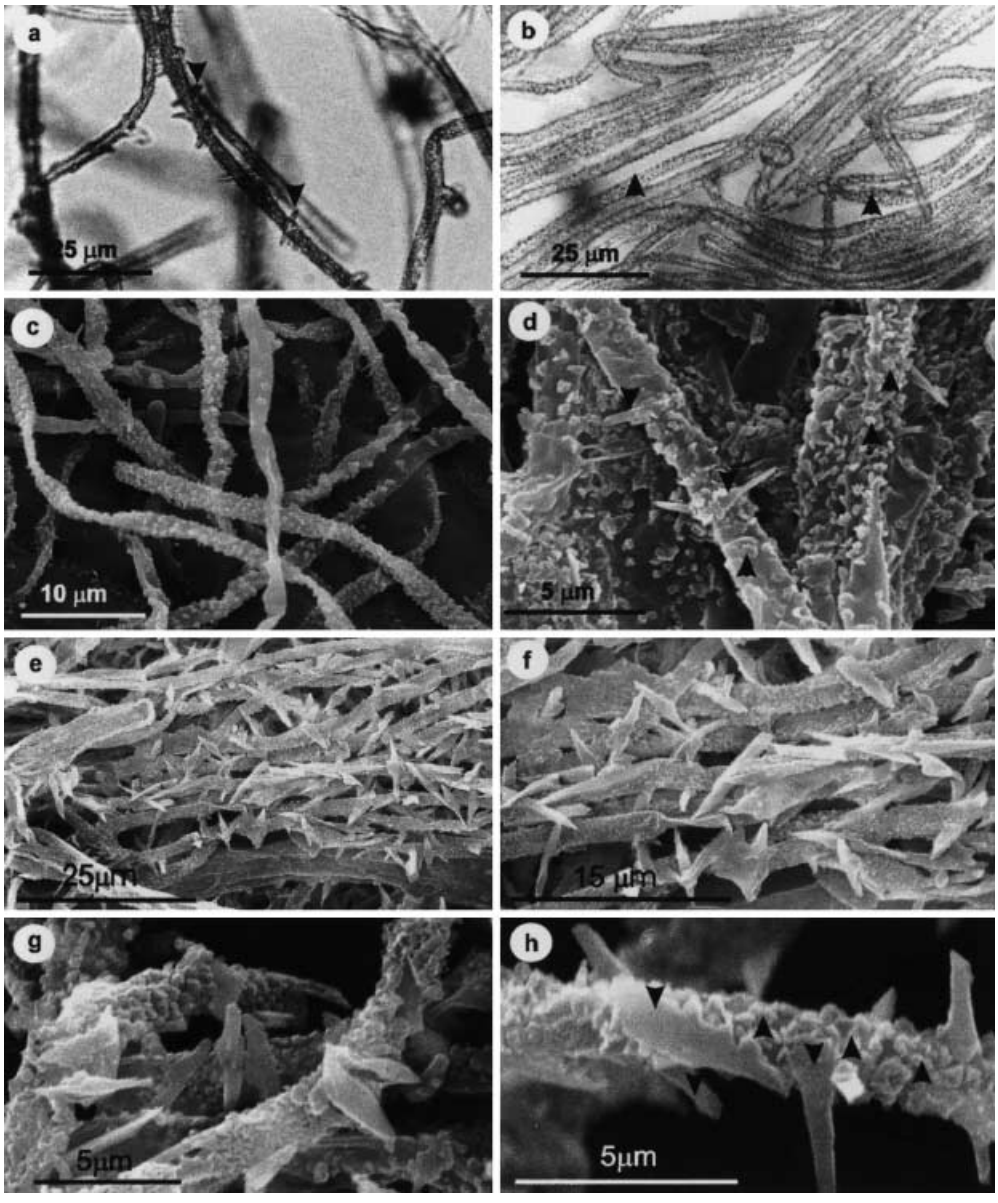

Fig. 1a–h Micrographs of encrustations of *Piloderma – Picea glauca* × *engelmannii*. *Up* and *down arrows* indicate verrucose and elongated crystals, respectively. **a** Light microscopy of a field sample showing elongated crystals; **b** light microscopy of a cultured sample showing verrucose encrustations; **c, d** scanning electron micrographs (SEM) of cultured samples showing both verrucose and elongated crystals; (**e–h**) SEM micrographs of field samples showing verrucose and elongated types of encrustations

Table 1 Mean chemical composition (weight percentage plus standard deviation; n=10) of hyphal encrustations of *Piloderma – Picea glauca* × *engelmanii* ectomycorrhizae in field and cultured samples determined by energy dispersive analysis. Across each row, means with different letters are significantly different (P<0.05)

Element	Elongated field	Verrucose field	Elongated cultured	Verrucose cultured
Carbon	21^{c} (12)	37^{b} (15)	51^{a} (6)	57^{a} (4)
Oxygen	57^{a} (13)	42^{b} (16)	35^{b} (6)	33^{b} (4)
Aluminum	2 (2)	<1	<1	<1
Silicon	2 (2)	1 (0.5)	2 (1)	2 (0.5)
Potassium	1 (1)	1 (1)	1 (1)	2 (2)
Calcium	17^{a} (6)	17^{a} (5)	7^{b} (2)	3^{b} (1)
Iron	<1	<1	1 (0.5)	<1

Chemical composition of encrustations

The FTIR absorption bands for the encrustations and the reference hydrated calcium oxalate crystals are shown in Fig. 3. Hydrated calcium oxalate had strong absorption bands at 600, 725, 781, 1257, 1623, and 3438 cm^{-1} and minor absorption at 516, 1445 and 1320 cm^{-1} wavenumbers. Encrustations on cultured and field samples had absorption bands similar to the reference crystals in addition to a strong absorption band between 1080 and 1017 cm^{-1} wavenumbers. Absorption bands at 3438 and 1623 cm^{-1} wavenumber represent the OH stretching vibration and the HOH deformation vibration of water, respectively (White and Roth 1986). The strong band at

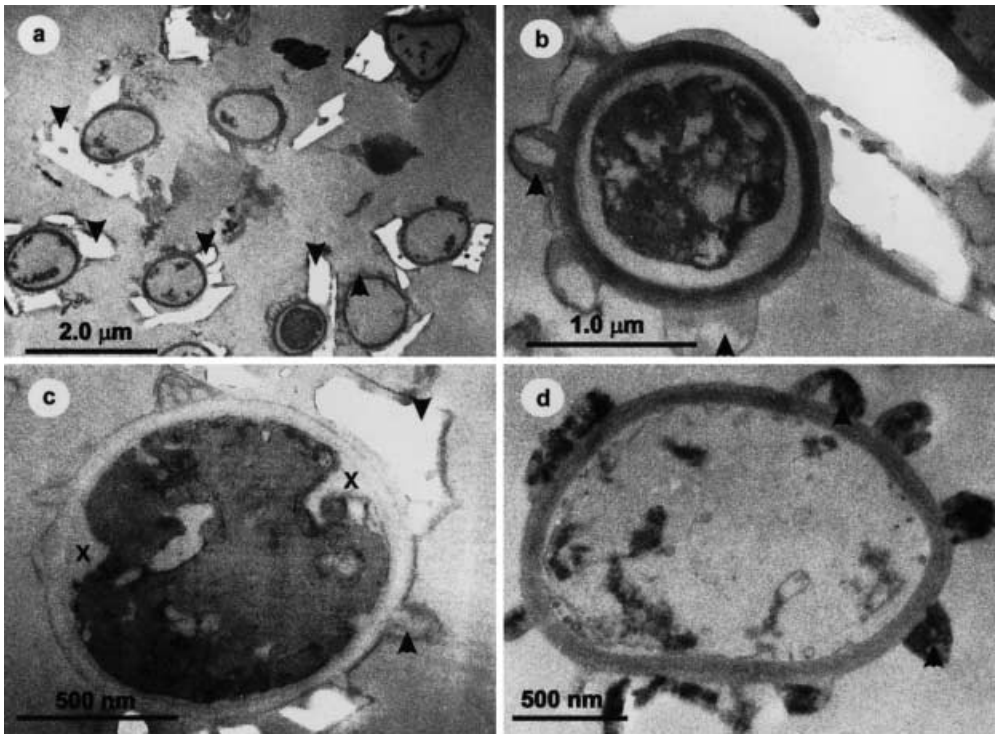

Fig. 2a–d Transmission electron micrographs of encrustations of *Piloderma – Picea glauca × engelmannii*. *Up* and *down arrows* indicate verrucose and elongated crystals, respectively. **a** Transverse sections of hyphae showing verrucose and elongated crystals (low magnification); **b** transverse sections of hyphae showing verrucose crystals (high magnification); **c** verrucose and elongated crystals and membrane body (*X*); **d** verrucose encrustations

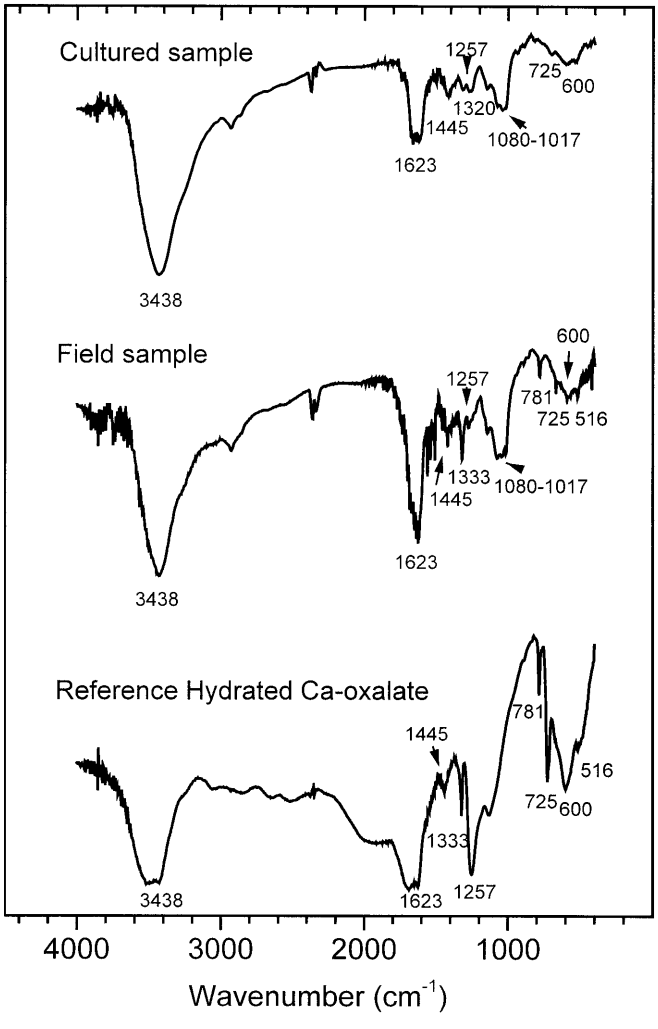

1445 cm^{-1} wavenumber represents the CH_3 deformation and the 1320-band represents CH bending vibration. The band at 1257 represents CaH_2 stretching vibration, and the 781, 725, and 600 bands are for CaO stretching vibrations. The absorption band at 516 cm^{-1} wavenumber results from HCaO bending vibration. The additional bands at 1080–1017 cm^{-1} wavenumbers in encrustations from field and cultured samples represent the C-O stretching vibration in polysaccharide (Stevenson 1994). Eger and Sücker (1964) assigned 1333 and 781 cm^{-1} wavenumbers as the major absorption bands for oxalate.

Discussion

Encrustations on hyphae of *Piloderma – Picea glauca × engelmannii* ECM are crystalline materials of distinct shapes and sizes predominantly comprising calcium oxalate. They are similar in composition but not in shape and size to crystals reported for other species of fungi (Cromack et al. 1979; Arnott and Webb 1983; Whitney and Arnott 1986a, b, 1987; Lapeyrie et al. 1990; Snetselaar and Whitney 1990; Jones et al. 1992; Connolly and Jellison 1994; Arnott 1995). In our study, crystals in *Piloderma* were verrucose, lenticular or elongated and <10 μm in size, in contrast to the crystals of *Resinicium bicolor*, which were commonly druses of twinned, styloid, crystals 5–40 μm in size (Connolly and Jellison 1994). Calcium oxalate deposits in *Agaricus bis-*

Fig. 3 Fourier-transformed infrared spectra of crystals of *Piloderma* from **a** a field sample, **b** a cultured sample, and **c** standard calcium oxalate reference crystals

porus ranged in shape from elongated rod-like to plate-like crystals (Whitney and Arnott 1986a).

Semi-quantitative SEM-EDS estimates of the calcium content of encrustations were relatively low when compared to the 27% calcium content of the reference monohydrated calcium oxalate CaC_2O_4-H_2O. The 17% calcium in crystals from field samples might indicate that calcium oxalate has at least six molecules of water in its structure. The lower calcium content in cultured samples than in field samples may be related to the stage of crystal formation or to the absence of plant roots. The high C and O contents in the crystals compared with the theoretical C and O contents of Ca-oxalate dihydrate may be attributed to the organic nature of the crystal sheath. This is consistent with Lapeyrie et al. (1990), who observed polysaccharide-rich materials covering calcium oxalate crystals on the hyphae of *Paxillus involutus*. The predominance of organic constituents in the crystal sheath may also explain the low calcium in verrucose crystals, which may have been at an earlier stage of crystal formation than the elongated crystals. With time, verrucose crystals may develop into euhedral elongated crystals. In *Agaricus bisporus* (Lge.) Sing., Eger and Sücker (1964) found amounts of calcium oxalate crystals ranging from high in young, small (<3 mm) fruitbodies to nearly absent from large, mature (>10 mm) fruitbodies.

The tangential occurrence of lenticular or elongated crystals on the surface of the verrucose type indicates the crystallization of the latter prior to the formation of the former. The precipitation of verrucose encrustations around the hyphae may be likened to the growth of crystals on the walls of soil pores attributed to crystal growth by secretion (Brewer 1976). This means that the solution containing calcium and oxalate may be secreted from the fungus cell onto the outside hypha wall, where it can grow into verrucose crystals. The similarity in cell wall composition and the "crystal sheath" suggests an intracellular origin of the calcium oxalate crystals and is consistent with previous reports (Frey-Wyssling 1981; Arnott 1982; Arnott and Webb 1983; Lapeyrie et al. 1990; Connolly and Jellison 1994). Most likely, crystal growth starts with the formation of the verrucose stage with a thick sheath. We hypothesize that the sheath thins as crystals develop into large euhedral lenticular and elongated crystals. Following complete crystal growth, part of the crystal sheath may rupture and dislodge the crystals into the soil environment. This mode of crystallization may explain our observation that the crystals were easily detached from the hyphae. The lenticular or elongated shapes observed in our study are similar to the oval-shaped crystal plaques found on sporangiophores of *Gilbertella persicaria* by Whitney and Arnott (1986b). These authors attributed the shape to water droplets that provided the "recrystallization fluid" containing calcium and oxalate needed to initiate the formation of encrustations.

Although our data do not directly explain the physiological function of calcium-rich encrustations, others suggest that calcium oxalate provides a hydrophobic coating preventing hyphae from becoming hydrated and thus reducing microbial attack (Whitney and Arnott 1986a, 1987). Crystals may also provide a physical barrier protecting the hyphae from predation by such organisms as grazing arthropods (Whitney and Arnott 1987). Connolly and Jellison (1994) proposed that calcium oxalate accumulation is a mechanism by which calcium is transported from sites of low to sites of high metabolic activity. Snetselaar and Whitney (1990) hypothesized that *Monotropa uniflora* ECM accumulate calcium oxalate to avoid potential calcium and oxalate toxicities. Recently, Jennings (1995) suggested that calcium oxalate production is important in the regulation of cytoplasmic pH as well as being a structural material of hyphae. In the future, we hope to characterize the contribution of hyphal encrustations to the supply of calcium and phosphorus for plant roots.

Acknowledgements We would like to acknowledge NSERC for financial support, Dr. D. Dick (University of Northern British Columbia) for FTIR analysis, Dr. M. Chen (University of Alberta) for assistance in TEM observations, and L. Tackaberry for valuable comments and suggestions.

References

Agerer R (ed) (1987–1998) Colour atlas of ectomycorrhizae. Einhorn, Schwäbisch Gmünd

Arnott HJ (1982) Calcium oxalate (Weddellite) crystals in forest litter. Scanning Electron Microsc 3:1141–1149

Arnott HJ (1995) Calcium oxalate in fungi. In: Khan S (ed) Calcium oxalate in biological systems. CRC, Boca Raton, Fla, pp 73–111

Arnott HJ, Webb MA (1983) The structure and formation of calcium oxalate crystal deposits on the hyphae of a wood rot fungus. Scanning Electron Microsc 4:1747–1758

Arocena JM, Glowa KR, Massicotte HB, Lavkulich L (1999) Chemical and mineral composition of ectomycorrhizosphere soils of subalpine fir (*Abies lasiocarpa* (Hook.) Nutt.) in the Ae horizon of a Luvisol. Can J Soil Sci 79:25–35

Brand F (1991) Ektomykorrhizen an *Fagus sylvatica* Charakterisierung und Identifizierung, ökologische Kennzeichnung und unsterile Kultivierung. Lib Bot 2:1–229

Brewer R (1976) Fabric and mineral analysis of soils, 2nd edn. Krieger, Huntington

Bullock PM, Fedoroff N, Jongerius A, Stoops G, Tursina T (1985) Handbook for soil thin section description. Waine Research, Wolverhampton

Connolly JH, Jellison J (1994) Calcium translocation, calcium oxalate accumulation, and hyphal sheath morphology in the white-rot fungus *Resinicium bicolor*. Can J Bot 73:927–936

Cromack K Jr , Sollins P, Grausten WC, Speidel K, Todd AW, Spycher G, Li CY, Todd RL (1979) Calcium oxalate accumulation and soil weathering in mats of the hypogeous fungus *Hysterangium crassum*. Soil Biol Biochem 11:463–468

Danielson RM (1984) Ectomycorrhizal association of jack pine stands in northern Alberta. Can J Bot 62:932–939

Danielson RM (1991) Temporal changes and effects of amendments on the occurrence of sheating (ecto-) mycorrhizas of conifers growing in oil sands tailings and coal spoil. Agric Ecosyst Environ 35:261–281

Dawson AG (1989) Soils of the Prince George-McLeod Lake area. Ministry of Environment Technical Report 29. Ministry of Agriculture and Fisheries, Victoria, BC, Canada

Eger G, Sücker I (1964) Besteht ein Zusammenhang zwischen Oxalatausscheidung und Fruchtkörperbildung beim Kultur-

champignon *Agaricus bisporus* (Lge.) Sing. Arch Mikrobiol 49:275–282
Frey-Wyssling A (1981) Crystallography of the two hydrates of crystalline calcium oxalate crystals in plants. Am J Bot 68: 130–141
Goodman DM, Trofymow JA (1996) *Piloderma fallax* (Libert) *Staplers +Pseudotsuga menziesii* (Mirb) Franco, CDE1. In: Goodman DM, Durall D, Trofymow JA, Berch SM (eds) Concise descriptions of North American ectomycorrhizae. Mycologue Publications and Canada-B.C. Forest Resource Development Agreement. Canadian Forest Service, Victoria, BC, Canada, pp CDE1.1–CDE1.4
Goodman DM, Trofymow JA (1998) Comparison of communities of ectomycorrhizal fungi in old-growth and mature stands of Douglas-fir at two sites on southern Vancouver Island. Can J For Res 28:574–581
Graustein WC, Cromack K Jr , Sollins P (1977) Calcium oxalate: occurrence in soils and effects on nutrient and geochemical cycles. Science 198:1252–1254
Ingleby K, Mason PA, Last FT, Fleming LV (1990) Identification of ectomycorrhizae. Institute of Terrestrial Ecology, Research Publication 5
Jennings DH (1995) The physiology of fungal nutrition. Cambridge University Press. Cambridge
Jones D, McHardy WJ, Wilson MJ, Vaughn D (1992) Scanning electron microscopy of calcium oxalate on mantle hyphae of hybrid larch roots from a farm forestry experimental site. Micron Microsc Acta 23:315–317
Jongmans A, Van Breemen N, Lundström U, van Hees PAW, Finlay RD, Srinivasan M, Unestam T, Giesler R, Melkerud PA, Olsson M (1997) Rock-eating fungi. Nature 389:682–683
Lapeyrie F, Picatto C, Gerard J, Dexheimer J (1990) TEM study of intracellular and extracellular calcium oxalate accumulation by ectomycorrhizal fungi in pure culture or in association with *Eucalyptus* seedlings. Symbiosis 9:163–166
Larsen MJ, Smith JE, McKay D (1997) On *Piloderma bicolor* and the closely related *P. byssinum*, *P. croceum*, and *P. fallax*. Mycotaxon 63:1–8
Marx DH (1969) Antagonism of mycorrhizal fungi to root pathogenic fungi and soil bacteria. Phytopathology 59:153–163
Massicotte HB, Peterson RL, Ackerly CA, Piché Y (1986) Structure of *Alnus crispa – Alpova diplophloeus* ectomycorrhizae. Can J Bot 64:177–192
Massicotte HB, Melville LH, Molina R, Peterson RL (1993) Structure and histochemistry of mycorrhizae synthesized between *Arbutus menziesii* (Ericaeae) and two basidiomycetes, *Pisolithus tinctorius* (Pisolithaceae) and *Piloderma bicolor* (Corticiaceae). Mycorrhiza 3:1–11
Massicotte HB, Melville LH, Peterson RL, Molina RL (1999) Biology of the ectomycorrhizal fungal genus *Rhizopogon*. IV. Comparative morphology and anatomy of ectomycorrhizas synthesized between several *Rhizopogon* species on ponderosa pine (*Pinus ponderosa*). New Phytol 142:355–370
Meidinger D, Pojar J, Harper WL (1991) Sub-boreal spruce zone. In: Meidinger D, Pojar J (eds) Ecosystems of British Columbia. Special Report Series No. 6. British Columbia Ministry of Forests, Victoria, BC, Canada, pp 209–221
Molina R, Massicotte HB, Trappe JM (1992) Specificity phenomena in mycorrhiza symbioses: community-ecological consequences and practical implications. In: Allen MF (ed) Mycorrhizal functioning, an integrative plant-fungal process. Routledge, Chapman and Hall, New York, pp 357–423
Nylund JE (1981) The formation of ectomycorrhizae in conifers: structural and physiological studies with special reference to the mycobiont *Piloderma croceum* Erikss. & Hjorts. PhD thesis, Uppsala University, Sweden
Nylund JE (1987) The ectomycorrhizal infection zone and its relation to acid polysaccharides of cortical cell walls. New Phytol 106:505–516
Nylund JE, Unestam T (1982) Structure and physiology of ectomycorrhizae. I. The process of mycorrhiza formation in Norway spruce in vitro. New Phytol 91:65–79
Paris F, Bonnaud P, Ranger J, Lapeyrie F (1994) Altération d'un phyllosilicate par des champignons ectomycorhiziens in vitro. Acta Bot Gallica 141:529–532
Paris F, Bonnaud P, Ranger J, Robert M, Lapeyrie F (1995a) Weathering of ammonium- or calcium-saturated 2:1 phyllosilicates by ectomycorrhizal fungi in vitro. Soil Biol Biochem 27: 1237–1244
Paris F, Bonnaud P, Ranger J, Lapeyrie F (1995b) In vitro weathering of phlogopite by ectomycorrhizal fungi. I. Effect of K^+ and Mg^{2+} deficiency on phyllosilicate evolution. Plant Soil 177:191–201
Paris F, Botton B, Lapeyrie F (1996) In vitro weathering of phlogopite by ectomycorrhizal fungi. II. Effect of K^+ and Mg^{2+} deficiency and N sources on accumulation of oxalate and H^+. Plant Soil 179:141–150
Snetselaar KM, Whitney KD (1990) Fungal calcium oxalate in mycorrhizae of *Monotropa uniflora*. Can J Bot 68:533–543
Statsoft (1995) Statistica for windows. Statsoft Inc., Tulsa, Okla
Stevenson FJ (1994) Humus chemistry: genesis, composition, reactions. Wiley, New York
Wallander H, Massicotte HB, Nylund JE (1997) Seasonal variation in protein, ergosterol and chitin in five morphotypes of *Pinus sylvestris* L. ectomycorrhiza in a mature Swedish forest. Soil Biol Biochem 29:45–53
White JL, Roth CB (1986) Infrared spectrometry. In: Klute A (ed) Methods of soil analysis, 2nd edn. Part 1. Physical and mineralogical methods. ASA-SSSA, Madison, Wis., pp 291–330
Whitney KD, Arnott HJ (1986a) Calcium oxalate crystals and basidiocarp dehiscence in *Geastrum saccatum* (Gasteromycetes). Mycology 78:649–656
Whitney KD, Arnott HJ (1986b) Morphology and development of calcium oxalate in *Gilbertella persicaria* (Mucorales). Mycology 78:42–51
Whitney KD, Arnott HJ (1987) Calcium oxalate crystal morphology and development in *Agaricus bisporus*. Mycology 79:180–187
Zak B (1976) Pure culture synthesis of Pacific madrone ectendomycorrhizae. Mycology 68:362–369